

Thermal weakening of cracks: a phase transition model

Tom Vincent-Dospital,^{1,*} Renaud Toussaint,^{1,2} Alain Cochard,¹ Knut Jørgen Måløy,² and Eirik G. Flekkøy²

¹*Institut de Physique du Globe de Strasbourg, UMR 7516 CNRS, Université de Strasbourg/EOST
5 rue René Descartes - F-67084 Strasbourg cedex, France*

²*Porelab, department of physics, University of Oslo
P. O. Box 1048, Blindern, N-0316 Oslo, Norway*

(Dated: December 15, 2024)

We present a model for the thermally activated propagation of cracks in elastic matrices. The propagation is considered as a subcritical phenomenon, the kinetics of which being described by an Arrhenius law. In this law, we take the thermal evolution of the crack front into account, assuming that a portion of the released mechanical energy is transformed into heat in a plastic process zone. We show that such a model leads to a two-phase crack propagation: a first phase at low velocity in which the temperature elevation is of little effect and the propagation is mainly governed by the mechanical load and by the toughness of the medium, and a second phase in which the crack is thermally weakened and propagates at greater velocity. Such a dual behavior can potentially explain the usual stick-slip in brittle fracturing, and we illustrate how with numerical simulations of mode I cracks propagating in thin disordered media. In addition, we predict the existence of a limiting ambient temperature above which the weakened phase ceases to exist and we propose this critical phenomenon as a novel explanation for the brittle-ductile transition of solids.

Of paramount importance in engineering and geophysics, the impact of temperature in fracturing processes have since long been studied. It can simplistically be sorted into two categories: background effects where the temperature is treated as an environmental constant affecting the rates at which the defects of a medium are propagating or healing [1–4] and dynamic effects where the propagation of fractures self-induces a rise in temperature in the vicinity of the crack front [5–8]. In the latter case, the heat elevation can be regarded as more than a secondary effect of the medium’s damage: it can be an active process back affecting the crack propagation. This phenomenon will be here referred to as “thermal weakening.” Such a weakening has notably been studied in earth science where it is believed to play a role in faults stability and earthquake triggering [9, 10] and it was included in the so-called rate-and-state framework [11] as an explanation for rate weakening faults. Several mechanisms have been proposed to explain thermal weakening, such as the melting of fracture surfaces or the thermopressurization of fault fluids [12–14]. We here present a model which disregards such effects and focuses on the statistical physics consideration of higher reactions rates (i.e., quicker fracture propagation) at higher temperatures, as implied by an Arrhenius law [15].

Such Arrhenius based models for the velocity of crack fronts have long been considered [1, 2, 4, 16] and have recently been shown to show good agreement with experimental observables of mode I cracks slowly propagating in acrylic glass bodies [17–19]. The rupture is then not considered as a Griffith-like threshold mechanism [20] where the crack only advances for $G > G_c$, where G is the energy release rate of the crack in J m^{-2} (arising from the mechanical load given to the crack front) and G_c the fracture energy of the medium (the energy bar-

rier per surface unit to overcome molecular bonds). It is rather considered as a thermally activated subcritical phenomenon ($G < G_c$) for which the crack velocity is expressed as:

$$V = \alpha \nu e^{-\frac{\alpha^2(G - G_c)}{k_b T}} \quad (1)$$

where α is the size (m) of the active microscopic breaking links, a characteristic length of the medium associated with the energy barrier of the fracturing process. $k_b \approx 1.38 \times 10^{-23} \text{ J K}^{-1}$ is the Boltzmann constant, T the absolute temperature at the crack tip and ν the thermal bath collisional frequency. Equation (1), as any Arrhenius law, is a continuous expression of a discrete process arising at the molecular scale. Cochard et al. [19] have recently discussed it at length. The exponential term is the probability (i.e. < 1) for the thermal agitation to exceed the activation energy $-\alpha^2(G - G_c)$ and hence for the crack to advance by a length α . This probability is challenged every $1/\nu$ seconds. In theory ν is also temperature dependent but this is of negligible effect compared to the exponential dependence of the probability term [15] and we hence define $V_0 = \alpha \nu$, the maximum crack velocity obtained when the activation energy is always reached. V_0 shall typically be in the range of the Rayleigh surface wave velocity [21]. Because we consider the thermal evolution around the crack tip we also note $T = T_0 + \Delta T$, where T_0 is the ambient temperature and ΔT any variation away from it at the tip.

This variation is induced by the dissipation of the mechanical energy given to the elastic matrix in a plastic zone around the crack tip [22]. Together with this Joule effect, other processes are responsible for some of this energy loss, such as the creation of new defects surfaces and the emission of mechanical waves. The model we use

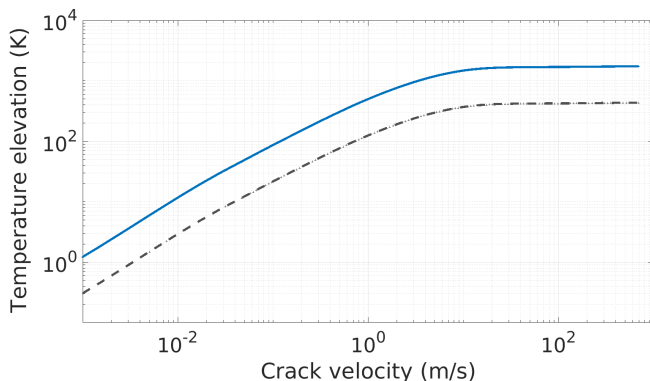


FIG. 1. Steady state values of the temperature elevation. It is obtained by solving Eq. (2) for a crack propagating at constant velocity and for $\phi G = 200 \text{ J m}^{-2}$ (plain plot) and $\phi G = 50 \text{ J m}^{-2}$ (dotted plot).

for the heat generation is based on the work of Toussaint et al. [8]: a portion ϕ of the energy release rate is dissipated on a cylindrical process zone of radius l centered around the crack tip. Such a configuration leads to a thermal evolution governed by:

$$\frac{\partial(\Delta T)}{\partial t} = \frac{\lambda}{C} \nabla^2(\Delta T) + \frac{\phi G V}{C \pi l^2} f \quad (2)$$

which is a diffusion equation including a source term. λ is the medium's thermal conductivity in $\text{J s}^{-1} \text{ m}^{-1} \text{ K}^{-1}$, C is the volumetric heat capacity in $\text{J K}^{-1} \text{ m}^{-3}$, t is the time variable and ∇^2 is the Laplace operator. f is the support function of the thermal process zone of surface integral πl^2 (i.e., $f = 1$ in the zone and $f = 0$ otherwise). Solving this equation for a crack propagating at a constant velocity and constant release rate, one can show that the thermal elevation at the tip reaches a steady state after a short transient time. Figure 1 shows the evolution of this steady state as a function of V and for two values of G . See the supplemental material for details on its computation. In our model, we use this relation to describe $\Delta T(V, G)$, thus discarding any transient regime. Equation (1) becomes:

$$V = V_0 e^{\frac{\alpha^2(G - G_c)}{k_b[T_0 + \Delta T(V, G)]}}. \quad (3)$$

Note that most of the previously introduced parameters are strongly dependent on the medium in which the crack propagates. The figures we display here use parameters we believe to be likely for the propagation of interfacial cracks in sintered PMMA bodies [17, 18] and are discussed in the supplemental material: $\alpha = 2.5 \times 10^{-11} \text{ m}$, $G_c = 250 \text{ J m}^{-2}$, $T_0 = 293 \text{ K}$, $C = 1.7 \times 10^6 \text{ J K}^{-1} \text{ m}^{-3}$, $\lambda = 0.19 \text{ J s}^{-1} \text{ m}^{-1} \text{ K}^{-1}$, $V_0 = 1000 \text{ m s}^{-1}$, $l = 20 \text{ nm}$ and $\phi = 1$.

Equation (3) defines, for a given load G , a function S_G

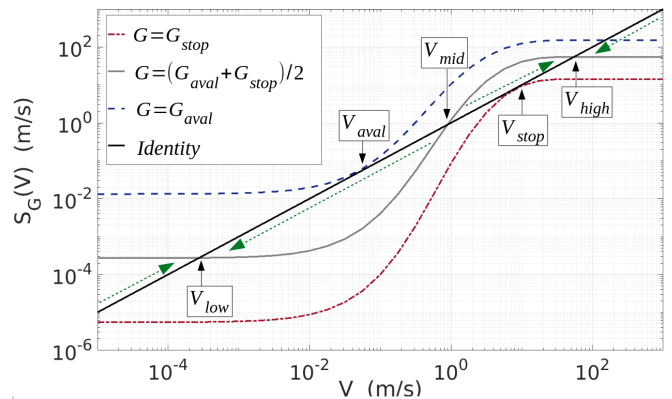


FIG. 2. Representation of $V = S_G(V)$ for three values of G : G_{stop} , G_{aval} ($> G_{\text{stop}}$) and the mid-value between G_{stop} and G_{aval} . The intersections of S_G with the identity plot (straight line) give the possible crack velocities. They are denoted V_{low} , V_{mid} and V_{high} and are emphasized for the intermediate G -plot. V_{aval} and V_{stop} are indicated on the two others plots. The dashed arrows indicate how off-balanced situations evolve to a stable fixed point.

such as: $V = S_G(V)$. To fit the model, the actual velocity at which a crack advances must be a solution of this equation (i.e., be a fixed point for the function S_G) [23]. Figure 2 illustrates that, depending on the value of G , S_G has one to three fixed points: three possible values for the crack velocity. This finite number of solutions arises from the steady-state approximation. If we were to consider the transient regimes, $S_G(V)$ would be, for a front propagating at any velocity V and load G , a target velocity. Any crack not having reached a steady state would thus accelerate or slow down to follow this function. The intermediate fixed point, when it exists, is then unstable (virtually impossible): a crack with a velocity value just above this point ($V < S_G(V)$) is too slow to be steady. The heat generation in the process zone is higher than what the diffusion can accommodate, the temperature rises and the velocity increases to converge to the upper fixed point. On the contrary, if a crack is slightly slower than the intermediate solution ($V > S_G(V)$), the crack cools down to the lower fixed point. We here assume that such transitions happen in a negligible time so the steady velocities are sufficient to describe the main dynamics. The outer solutions of (3) being the only stable ones, the model displays a two-phase behavior. The lower velocity marks a slow phase. The temperature elevation at the crack tip has little effect on the propagation, as $\Delta T(V, G) \ll T_0$. The higher solution corresponds to a thermally weakened phase where $\Delta T(V, G)$ has reached the plateau temperature of Fig. 1. The velocity is there increased as the induced heat is potentially significant compared to the thermal background.

Notice in Fig. 2 that there are two particular values of the load G for which either the lower or the higher phase ceases to exist. We denote them G_{aval} and G_{stop} (with

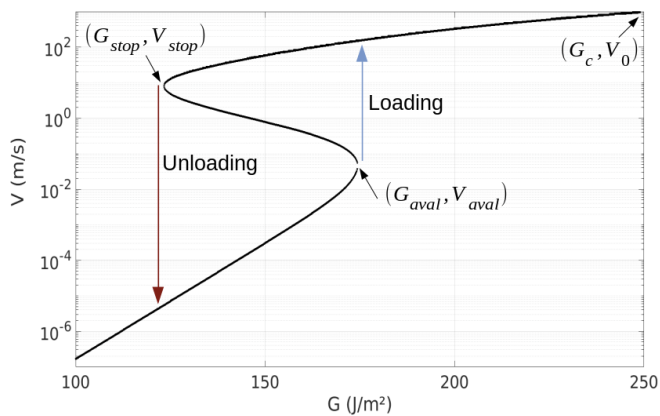


FIG. 3. Solutions for the crack velocity as a function of G for $T_0 = 293$ K. All solutions in between V_{stop} and V_{aval} are unstable, any other point is a possible crack velocity. The arrows represent how a crack avalanches or slows down at the phase transition thresholds.

$G_{\text{aval}} > G_{\text{stop}}$) as they correspond to mechanical loads at which a slow crack will have to avalanche to the thermally weakened phase or at which a fast (weakened) crack can only cool down to the slow phase. For G in between these two thresholds, a hysteresis situation holds, there are several solutions for V and the crack might or might not be thermally weakened, depending on the mechanical history. To G_{aval} and G_{stop} correspond some specific velocities $V_{\text{aval}} < V_{\text{stop}}$ in between which a crack cannot propagate, as any solution is there unstable. Figure 3 shows the possible crack velocities for various values of G . One can notice how similar it is to a first order phase transition [24] for the order parameter V associated to avalanches (jumps in V) triggered by variations in the driving field G at temperature T_0 . In the hysteresis domain, our model does not discriminate on the relative stability of each phase. One could however argue by analogy with other phase transition systems [24], that one of the two solutions could only be metastable, that is, in an equilibrium which is less energetically favorable than the one of the alternative phase. In this case, when traveling through an heterogeneous medium where the variations in fracture energy are enough to get shifts from only one state to the other, one of the phase could still be preferential for the crack propagation.

Besides G , T_0 is the only other parameter of (3) which is not dependent on the medium's properties. Figure 4 thus shows the predicted propagation velocities for various ambient temperatures. Notice the existence of a critical ambient temperature: T_0^* , at which $G_{\text{aval}} = G_{\text{stop}} = G^*$ and $V = V^*$. Beyond T_0^* , the Joule effect cannot overcome the thermal background enough for the crack to be weakened. Increasing the load then only leads to a smooth increase in the velocity. To relate to the theory of critical phenomena in phase transitions [24] we looked

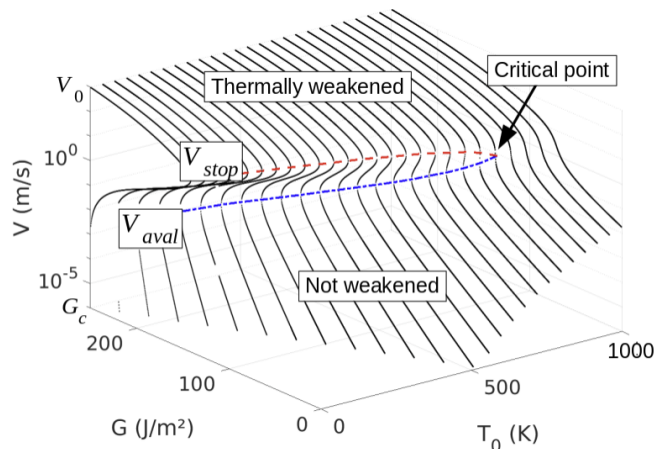


FIG. 4. Solutions for the crack velocity as a function of G and for various T_0 . The dashed lines show the $(V_{\text{stop}}, G_{\text{stop}})$ and $(V_{\text{aval}}, G_{\text{aval}})$ couples and converge to the critical point.

for the real numbers β , δ and γ such that:

$$\frac{V - V^*}{V^*} \sim \left(\frac{T_0 - T_0^*}{T_0^*} \right)_{G=G^*}^{\beta} \quad (4)$$

$$\frac{G - G^*}{G^*} \sim \left(\frac{V - V^*}{V^*} \right)_{T_0=T_0^*}^{\delta} \quad (5)$$

$$\frac{G^*}{V^*} \frac{\partial V}{\partial G} \sim \left(\frac{T_0 - T_0^*}{T_0^*} \right)_{G=G^*}^{-\gamma} \quad (6)$$

where \sim stands for a mathematical equivalence in the vicinity of the critical point (any pre-factor is overlooked). These exponents describe how V converges towards V^* beyond the critical point ($T_0 \geq T_0^*$). We also characterized how the hysteresis domain shrinks, looking for β' , δ' and γ' such that:

$$\frac{V_{\text{stop}} - V_{\text{aval}}}{V^*} \sim \left(\frac{T_0^* - T_0}{T_0^*} \right)^{\beta'} \quad (7)$$

$$\frac{G_{\text{aval}} - G_{\text{stop}}}{G^*} \sim \left(\frac{V_{\text{stop}} - V_{\text{aval}}}{V^*} \right)^{\delta'} \quad (8)$$

$$\frac{G^*}{V^*} \frac{V_{\text{stop}} - V_{\text{aval}}}{G_{\text{aval}} - G_{\text{stop}}} \sim \left(\frac{T_0^* - T_0}{T_0^*} \right)^{-\gamma'} \quad (9)$$

With a bisection, we numerically estimated the critical point, checking for the number of solutions of $V = S_G(V)$ (three solutions below T_0^* and one above). Analyzing the shape of the velocity map in the derived vicinity we found: $\beta \approx 1/3$, $\delta \approx 3$, $\gamma \approx 2/3$, and $\beta' \approx 1/2$, $\delta' \approx 3$,

$\gamma' \approx 1$ (see supplemental material). Both sets of exponents respect the scaling relation [24]: $2\beta + \gamma = \beta(\delta + 1)$. We hence derived critical exponents which are, along the phase co-existence domain, the same as the mean field exponents for, say, the liquid-gas transition [24], but different beyond the critical point. The mean field characteristic might arise from the statistical nature of the Arrhenius law only representing an average velocity while consecutive molecular bonds can be overcome at very different speeds. Another interpretation is that it translates the 1D character of our model. We have indeed disregarded any velocity variations and elastic interactions along the crack front, making the assumption that it is thin or symmetrical enough perpendicularly to the propagation direction.

Let us finally illustrate the phase transitions with some simulations of such unidimensional fronts loaded in mode I. The loading geometry that we consider is shown in Fig. 5. The support body consists in two sintered elastic plates which are progressively separated at the edge. The deflection on the side, $u(t)$ (in m), is increased linearly with time: $u(t) = v_u t$. Using the Euler–Bernoulli beam theory [25], one can compute the energy release rate at the tip of such a system:

$$G(t) = \frac{3Eh^3v_u^2t^2}{8a(t)^4} \quad \text{if } a \gg h, \quad (10)$$

with E the body Young modulus (in Pa), h half of its thickness and a the crack advancement such as: $V = \partial a / \partial t$. By inserting (10) in (3), we obtain the differential equation in $a(t)$ that governs the crack progression and that we solved with a time step adaptive Runge-Kutta algorithm [26]. We here consider a crack interface with a homogeneous background cohesion $G_c = G_{cb}$ which is only disturbed by a single tough asperity of length L_a ($G_{ca} > G_{cb}$). Figure 5 shows a schematic for this anomaly while Fig. 6 shows, for several values of G_{ca} , the course of the crack over it and the corresponding evolution of the energy release rate. When the front reaches the asperity, the crack velocity dramatically decreases as it reaches a tougher area. Meanwhile the load G increases because the far field deflection continues to build up on a now quasi-static crack. Once the anomaly finally gets passed, the simulations show two possible scenarios. If $G_{\text{aval}}(G_{cb})$ (i.e., the phase shift threshold for the background G_{cb}) was not reached over the anomaly, then the crack only accelerates back to its pre-asperity state. However, if $G_{\text{aval}}(G_{cb})$ was overcome, the crack shifts phase and becomes thermally weakened: it avalanches until $G = G_{\text{stop}}$. In Fig. 6, one can read the values of G_{aval} and G_{stop} and remark that they match the theoretical values displayed in Fig. 3. Note that, if the load was to be quickly increased, an avalanche could be triggered without the need for any asperity. We showed, however, how the medium's disorder can lead to some spontaneous thermal weakening of the crack course.

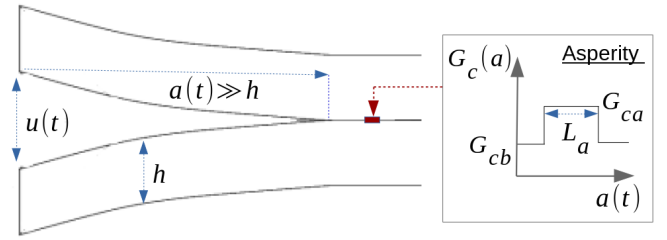


FIG. 5. Geometry for the numerical simulations of unidimensional crack fronts overcoming a tough asperity.

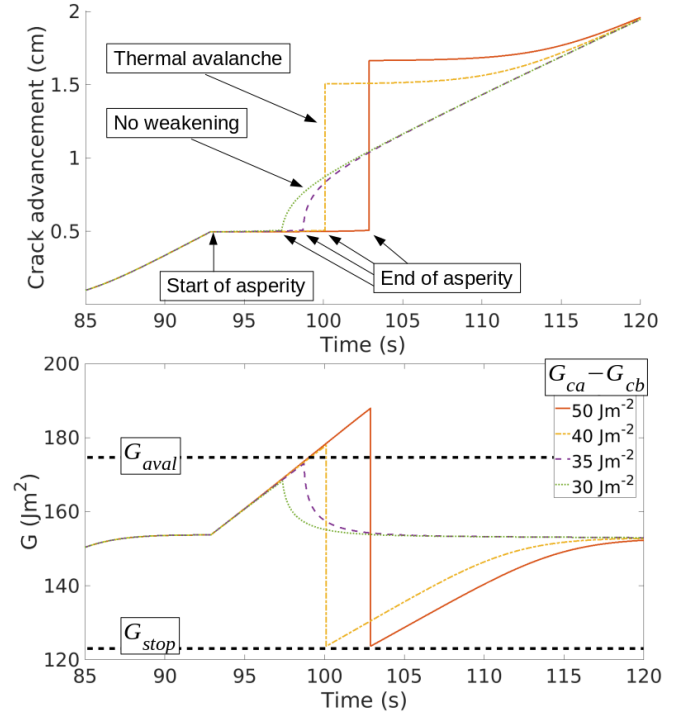


FIG. 6. Numerical simulations for a crack overcoming an asperity as defined by the differential equation from (3) and (10) and for various G_{ca} . $L_a = 100 \mu\text{m}$, $v_u = 120 \mu\text{m s}^{-1}$, $h = 5 \text{ mm}$ and $E = 3.2 \text{ GPa}$. The top plot is the crack advancement $a(t)$, the bottom one is the energy release rate $G(t)$. Thermal weakening is or is not triggered depending on the anomaly strength.

By combining an Arrhenius law and the heat equation, we have thus demonstrated the possibility of a thermally activated dynamic phase transition in the propagation of cracks. This phase description may have major implications for the understanding of fracture dynamics. With a rather simple subcritical model, we indeed explain both slow creep regimes and fast ruptures. We do not however strictly disregard over-critical propagations, as $G > G_c$ only implies that the Arrhenius activation energy is null and hence always exceeded. In this case, we predict $V \sim V_0$. For such high velocities, we derive tip temperatures approaching the 10^4 K range. This temperature only stands on small volumes ($\sim l^3$) and short

periods ($\sim l/V$) such that it does not imply a gigantic level of energy nor it necessarily leads to local fusion or sublimation of the solid. Note that the temperature merely measures the amplitude of the atoms agitation, and that its statistical definition actually suffers for process zones smaller than the molecular scale. Besides describing the two phases, we explained the potential shifts from one to the other and point out here how compatible this is with the usual stick-slip in brittle fracturing processes [16, 27], when avalanches get considerably larger than the scales of the in situ quenched disorder. We also showed that above a critical ambient temperature, T_0^* , this phenomenon cannot occur. For materials where T_0^* is lower than the melting point at a given confining pressure, a same solid then displays a different behavior under cool or hot conditions: fragile when cold, but smoother/ductile when warm, as thermal avalanches are inhibited. Our model thus stands as a novel and physical explanation for the fragile-ductile transition of matter. Finally, and although we presented a mode I model, we suggest that some analogy is to be made with the frictional effects induced in mode II and mode III fracturing. Notably, as frictional heating is believed to be a cause for the instability of some seismic faults, a potential earthquake triggered when overcoming a strong fault plane asperity might indeed be amplified due to thermal weakening. The existence of the critical point would then explain the disappearance of such amplifications at higher depth (i.e., where rocks are in ductile conditions [28]) as the thermal background is there enough to make the frictional heating negligible and, hence, favors creep over brittle ruptures.

Acknowledgement and information

T.V.-D. developed and analyzed the model and the simulations, and redacted the first versions of the manuscript. R.T. proposed the physical basis of the model and its mathematical formulation. A.C. set the basis for the numerical implementation of the model and the principles of the resolution algorithm. K.J.M. contributed in the interpretation of the model in fracture mechanics applications. E.G.F. contributed to analyze the model in terms of critical point characteristics. All authors participated to the redaction of the manuscript and agreed with the submitted version. They declare no competing financial interests in the publishing of this work and acknowledge the support of the LIA France-Norway D-FFRACT, of the Universities of Strasbourg and Oslo and of the CNRS INSU ALEAS program. Readers are welcome to comment and should address to vincentdospitalt@unistra.fr. See Supplemental Material below for a discussion on the parameters we used, details on how to compute the temperature elevation at the crack tip and decades on which we fitted the critical

exponents.

* vincentdospitalt@unistra.fr

- [1] S. S. Brenner. Mechanical behavior of sapphire whiskers at elevated temperatures. *Journal of Applied Physics*, 33(1):33–39, 1962. doi:10.1063/1.1728523.
- [2] S. N. Zhurkov. Kinetic concept of the strength of solids. *International Journal of Fracture*, 26(4):295–307, Dec 1984. ISSN 1573-2673. doi:10.1007/BF00962961.
- [3] N. Brantut, M. J. Heap, P. G. Meredith, and P. Baud. Time-dependent cracking and brittle creep in crustal rocks: A review. *Journal of Structural Geology*, 52:17–43, 2013. ISSN 0191-8141. doi:10.1016/j.jsg.2013.03.007.
- [4] B. Lawn. *Fracture of Brittle Solids*. Cambridge Solid State Science Series. Cambridge University Press, 2 edition, 1993. doi:10.1017/CBO9780511623127.
- [5] J. R. Rice and N. Levy. Local heating by plastic deformation at a crack tip. *Physics of Strength and Plasticity*, pages 277–293, 1969.
- [6] K. N. G. Fuller, P. G. Fox, and J. E. Field. The temperature rise at the tip of fast-moving cracks in glassy polymers. *Proceedings of the Royal Society of London A: Mathematical, Physical and Engineering Sciences*, 341(1627):537–557, 1975. ISSN 0080-4630. doi:10.1098/rspa.1975.0007.
- [7] G. Pallares, C. L. Rountree, L. Douillard, F. Charra, and E. Bouchaud. Fractoluminescence characterization of the energy dissipated during fast fracture of glass. *Europhysics Letters*, 99(2):28003, 2012.
- [8] R. Toussaint, O. Lengliné, S. Santucci, T. Vincent-Dospital, M. Naert-Guillot, and K. J. Måløy. How cracks are hot and cool: a burning issue for paper. *Soft Matter*, 12:5563–5571, 2016. doi:10.1039/C6SM00615A.
- [9] S. Braeck and Y. Y. Podladchikov. Spontaneous thermal runaway as an ultimate failure mechanism of materials. *Phys. Rev. Lett.*, 98:095504, Mar 2007. doi:10.1103/PhysRevLett.98.095504.
- [10] J. R. Rice. Heating and weakening of faults during earthquake slip. *Journal of Geophysical Research: Solid Earth*, 111(B5), 2006. doi:10.1029/2005JB004006.
- [11] H. Noda, E. M. Dunham, and J. R. Rice. Earthquake ruptures with thermal weakening and the operation of major faults at low overall stress levels. *Journal of Geophysical Research: Solid Earth*, 114(B7). doi:10.1029/2008JB006143.
- [12] A. W. Rempel and J. R. Rice. Thermal pressurization and onset of melting in fault zones. *Journal of Geophysical Research: Solid Earth*, 111(B9), 2006. doi:10.1029/2006JB004314.
- [13] C. Wibberley and T. Shimamoto. Earthquake slip weakening and asperities explained by fluid pressurization. 436:689–92, 09 2005.
- [14] J. Sulem and V. Famin. Thermal decomposition of carbonates in fault zones: Slip-weakening and temperature-limiting effects. *Journal of Geophysical Research: Solid Earth*, 114(B3). doi:10.1029/2008JB006004.
- [15] G. G. Hammes. *Principles of Chemical Kinetics*. Academic Press, 1978. ISBN 978-0-12-321950-3. doi:doi.org/10.1016/B978-0-12-321950-3.50005-0.

- [16] S. Santucci, L. Vanel, and S. Ciliberto. Subcritical statistics in rupture of fibrous materials: Experiments and model. *Phys. Rev. Lett.*, 93:095505, Aug 2004. doi: 10.1103/PhysRevLett.93.095505.
- [17] O. Lengliné, R. Toussaint, J. Schmittbuhl, J. E. Elkhoury, J. P. Ampuero, K. T. Tallakstad, S. Santucci, and K. J. Måløy. Average crack-front velocity during subcritical fracture propagation in a heterogeneous medium. *Phys. Rev. E*, 84:036104, Sep 2011. doi: 10.1103/PhysRevE.84.036104.
- [18] K. T. Tallakstad, R. Toussaint, S. Santucci, J. Schmittbuhl, and K. J. Måløy. Local dynamics of a randomly pinned crack front during creep and forced propagation: An experimental study. *Phys. Rev. E*, 83:046108, 04 2011.
- [19] A. Cochard, O. Lengliné, K. J. Måløy, and R. Toussaint. Thermally activated crack fronts propagating in pinning disorder: simultaneous brittle/creep behavior depending on scale. *Philosophical Transactions of the Royal Society A : Mathematical, Physical and Engineering Sciences*, 2018. doi:10.1098/rsta.2017.0399.
- [20] A. Griffith. The Phenomena of Rupture and Flow in Solids. *Philosophical Transactions of the Royal Society of London A: Mathematical, Physical and Engineering Sciences*, 221(582-593):163–198, January 1921. ISSN 1471-2962. doi:10.1098/rsta.1921.0006.
- [21] L. B. Freund. Crack propagation in an elastic solid subjected to general loading. *Journal of the Mechanics and Physics of Solids*, 20(3):129 – 152, 1972. ISSN 0022-5096. doi:10.1016/0022-5096(72)90006-3.
- [22] G. R. Irwin. Analysis of stresses and strains near the end of a crack traversing a plate. *Journal of Applied Mechanics*, 24:361–364, 1957.
- [23] D. K. Arrowsmith and C. M. Place. *An introduction to dynamical systems*. Cambridge University Press, 1990.
- [24] H. B. Callen. *Thermodynamics and an Introduction to Thermostatistics*, volume 55. 1987.
- [25] T. L. Anderson. *Fracture Mechanics: Fundamentals and Applications*. Taylor and Francis, 2005.
- [26] J. R. Dormand and P. J. Prince. A family of embedded Runge-Kutta formulae. *Journal of Computational and Applied Mathematics*, 6(1):19 – 26, 1980. ISSN 0377-0427. doi:10.1016/0771-050X(80)90013-3.
- [27] M.-J. Dalbe, S. Santucci, P.-P. Cortet, and L. Vanel. Strong dynamical effects during stick-slip adhesive peeling. *Soft Matter*, 10:132–138, 2014. doi: 10.1039/C3SM51918J.
- [28] C. H. Scholz. The brittle-plastic transition and the depth of seismic faulting. *Geologische Rundschau*, 77(1):319–328, Feb 1988. ISSN 1432-1149. doi: 10.1007/BF01848693.

Thermal weakening of cracks: a phase transition model

SUPPLEMENTAL MATERIAL

Tom Vincent-Dospital,^{1,*} Renaud Toussaint,^{1,2} Alain Cochard,¹ Knut Jørgen Måløy,² and Eirik G. Flekkøy²

¹*Institut de Physique du Globe de Strasbourg, UMR 7516 CNRS, Université de Strasbourg/EOST
5 rue René Descartes - F-67084 Strasbourg cedex, France*

²*Porelab, department of physics, University of Oslo
P. O. Box 1048, Blindern, N-0316 Oslo, Norway*

(Dated: December 15, 2024)

In this supplemental material, we explain the parameters that we used for illustration in the main manuscript. We also provide analytical approximations for the temperature elevation at the crack tip and details how the critical exponents were derived. Although it is not essential to the core comprehension of our letter, we do refer to it. Therefore, for an easier understanding of the present material, we invite the reader to keep an eye onto the main manuscript, which references are marked with a ‘M’. For instance: Eq. (M1).

CONTENTS

I. Chosen parameters (for illustration)	1
II. Temperature elevation at the crack tip	2
A. Analytical approximation	2
B. Transient time	3
III. More on the critical point	3
References	4

I. CHOSEN PARAMETERS (FOR ILLUSTRATION)

Most of the parameters that we introduced in our model are strongly dependent on the medium in which the crack propagates. The chosen ones, for the figures of the main manuscript, use values we believe to be likely for the propagation of interfacial cracks in sintered poly-methyl methacrylate (PMMA) bodies [1, 2]. Tallakstad et al. [2] have derived the main parameters of the Arrhenius law with experiments done at room temperature and for slow crack growth such that it is unlikely that a significant heat was released at the crack tip. In this experiments, V was indeed reported to increase exponentially with G , meaning that $\Delta T(V, G)$ is negligible in Eq. (M3). They found $\alpha \sim 2.5 \times 10^{-11}$ m which is surprisingly less than the typical size of molecular bonds, one Ångström. It was proposed, as a possible explanation, that it is a consequences of the off-plane processes in the advance of a crack (a number of off-plane bonds have to be broken for the planar interface to advance by a projected length α). A nominal velocity $V_0 \times \exp[-\alpha^2 G_c / (k_b T_0)]$ was also measured, although the contributions of V_0 and G_c were not individually resolved. We however used $V_0 = 1000$ m s⁻¹, of the order of magnitude of the Rayleigh wave velocity [3] (≈ 1280 m s⁻¹ in Plexiglas [4]). This leads to $G_c = 250$ J m⁻². Note that to relate to the probabilistic molecular description of the Arrhenius law, one could also consider V_0 as the average molecular velocity from the kinetics theory [5]. If we approximate it as for uni-molecular gas, $V_0 \sim \sqrt{8k_b T_0 / (\pi m)}$ where m is the mass of a molecule), it ranges from 100 to 1000 m s⁻¹ for molecular masses from 100 g mol⁻¹ (MMA molecule scale) to 10 g mol⁻¹ (atomic scale). Typical thermal constants for the Plexiglas were chosen as per the manufacturer specifications [6]: $C = 1.7 \times 10^6$ J K⁻¹ m⁻³ and $\lambda = 0.19$ J s⁻¹ m⁻¹ K⁻¹. Finally, we chose a process zone radius of $l = 20$ nm corresponding to the scale of a few methyl methacrylate units, and we assume for simplicity that $\phi = 1$: most of the energy contributes to the Joule effect and the other dissipation processes are comparatively negligible.

* vincentdospitalt@unistra.fr

II. TEMPERATURE ELEVATION AT THE CRACK TIP

As stated in the main manuscript, the temperature evolution at the moving crack tip is dictated by the following equation:

$$\frac{\partial(\Delta T)}{\partial t} = \frac{\lambda}{C} \nabla^2(\Delta T) + \frac{\phi G V}{C \pi l^2} f \quad (1)$$

which is a diffusion equation including a source term. f is the support function of the thermal process zone of surface integral πl^2 (we used $f = 1$ in the zone and $f = 0$ otherwise). It can notably be solved for the tip temperature using the diffusion Green's function [7]:

$$\Delta T(t) = \int_{-\infty}^t dt' \iiint_{PZ(t')} dv \frac{\phi G V}{C \pi l^2} \frac{e^{-\frac{C r^2}{4 \lambda (t-t')}}}{\left[\frac{4 \pi \lambda}{C} (t-t')\right]^{\frac{3}{2}}} \quad (2)$$

$$\text{with } r = r(\mathbf{dr}, t', t) = \left\| - \int_{t'}^t \mathbf{V} dt'' + \mathbf{dr} \right\|$$

where dv is the volume of an elementary heat source of the advancing process zone (PZ). This source is, at time t' , located at a distance r from the crack tip at time t . We denote \mathbf{dr} the positioning vector from the PZ center to the elementary source. See Fig. 1 for an illustration of these parameters. The time integration of (2) adds up the whole history of sources position, while the volumetric integral sums the contribution, for a given time t' , of infinitesimal heat sources of the process zone.

The steady state which we used in our model is then the limit of $\Delta T(t)$ for large times ($t \rightarrow +\infty$), assuming V and G are constant.

A. Analytical approximation

For constant crack velocity and energy release rate, the temperature elevation at the steady state can be approximated [8]. When the crack propagates slowly, the temperature at the crack tip is constrained by the diffusion process. The process zone dissipates an energy $\phi G V \tau_0 dh$ during the time $\tau_0 = l/V$ that it has spent over the tip location. dh is the length of a crack front element. This energy is diffused over a roughly cylindrical volume with radius equal to the skin depth of diffusion δ over the time τ_0 . The section of such a cylinder is given by $\pi \delta^2 \approx \lambda \tau_0 / C$, leading to:

$$\Delta T_{\text{slow}} = \frac{(\phi G V \tau_0 dh)}{C(\pi \delta^2 dh)} = \phi G \frac{V}{\lambda}. \quad (3)$$

In this case, because of the small velocity, l is small compared to δ . However, for cracks propagating fast enough $\delta \ll l$. The diffusion is then negligible and all of the

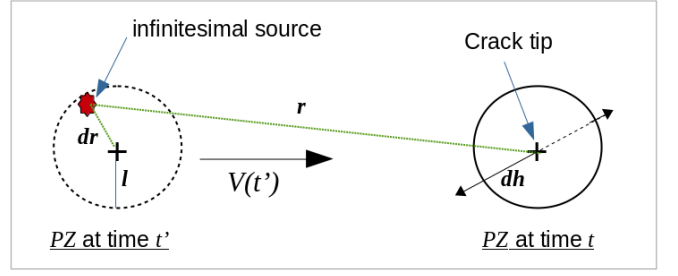


FIG. 1. Illustration of the geometric parameters used in Eq. (2). dh is perpendicular to the figure perspective.

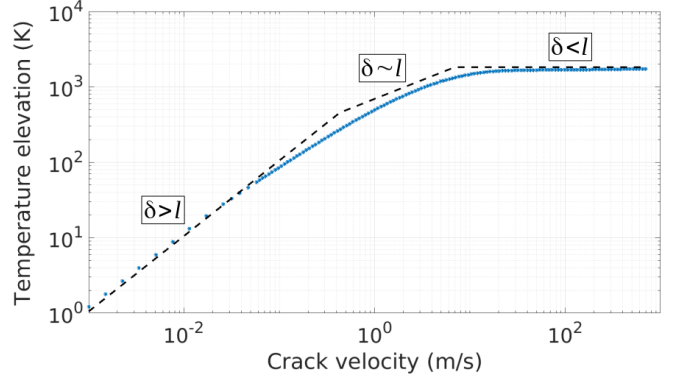


FIG. 2. Steady state values of the temperature elevation (blue dots) obtained by solving the diffusion equation (1) for a crack propagating at constant velocity for $\phi G = 200 \text{ J m}^{-2}$. The plotted asymptotes are the approximations (pre-factors included) from Eq. (3) to Eq. (5).

energy stays in the process zone of section πl^2 :

$$\Delta T_{\text{fast}} = \frac{(\phi G V \tau_0 dh)}{C(\pi l^2 dh)} = \frac{\phi G}{\pi C l}. \quad (4)$$

Note that ΔT_{fast} is the actual temperature at which the tip evolves in the weakened phase. Finally when $\delta \sim l$, the dissipated energy can only diffuse away from the process zone perpendicularly to the crack motion [8] and is spread over an ellipsoidal cross-section $\pi(\delta+l)l \approx 2\pi\delta l$, such as:

$$\Delta T_{\text{mid}} = \frac{(\phi G V \tau_0 dh)}{C(2\pi\delta l dh)} = \phi G \sqrt{\frac{V}{4\pi C \lambda}}. \quad (5)$$

Fig. 2 illustrate the validity of these three approximations, showing the full solution of the diffusion equation (1) together with asymptotes (3) to (5). We show that, for slow cracks, the temperature increases linearly with the propagation velocity. At higher V , it however reaches a plateau constrained by the size of the process zone.

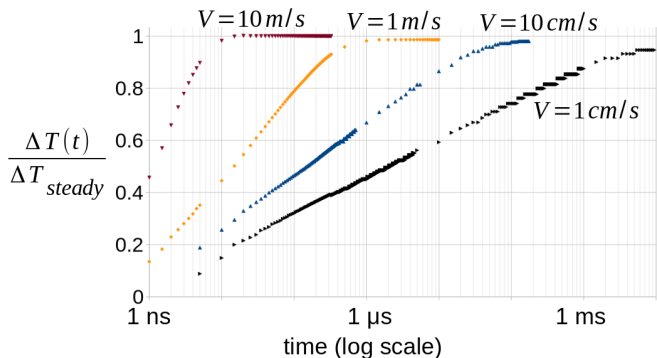


FIG. 3. Transient response for the heating of a crack propagating at constant V and G . The ratio of the tip temperature elevation and its steady state is shown for various velocities. One can read the actual value of ΔT_{steady} in Fig. 2.

B. Transient time

Let us consider a tip which does not move before $t_0 = 0$ s and propagates at velocity V and energy release rate G afterwards. Similarly to the steady state temperature, the transient time for its rise in temperature, τ , is velocity dependent. For a fast propagating crack, the heat is not effectively evacuated away from the process zone. The transient time then only corresponds to the maximum duration that the tip position stays in the plastic zone: $\tau_{\text{fast}}(V) \sim l/V = \tau_0$. For a slow crack, however, the characteristic time of the heat diffusion is to be considered. We can derive it by writing in Eq. (2) that $r \sim V(t-t')$. The heat kernel then behaves as $\exp[-(t-t')/\tau_{\text{slow}}]$ with $\tau_{\text{slow}}(V) \sim 4\lambda/(CV^2)$.

The quicker the crack progression, the shorter the thermal transient time. This is actually of convenience for our steady state approximation. For hot cracks, say propagating at velocities higher than 10 m s^{-1} (see Fig. 2), we have $\tau_{\text{fast}} < 10^{-9} \text{ s}$. For slower cracks however, say $V = 1 \text{ cm s}^{-1}$, τ_{slow} gets in the millisecond range. In this case we have $\Delta T \ll T_0$ and the Joule heating can anyway be neglected. The transient regimes for various velocities are displayed in Fig. 3 for illustration. This discussion is of course parameter dependent and one should keep in mind that our model is an approximation that could hold more or less for different parameters values.

III. MORE ON THE CRITICAL POINT

We ran a bisection to numerically estimate the position of the critical point (CP). This bisection checked, for any temperature T_0 , the maximum number of solutions of $V = S_G(V)$ to decide whether $T_0 > T_0^*$ (a unique solution for any G) or $T_0 < T_0^*$ (three solutions in the hysteresis domain). Numerical errors in this decision process imply some inaccuracy on the derived critical point. This, in return, leads to poorly determined critical exponents, as

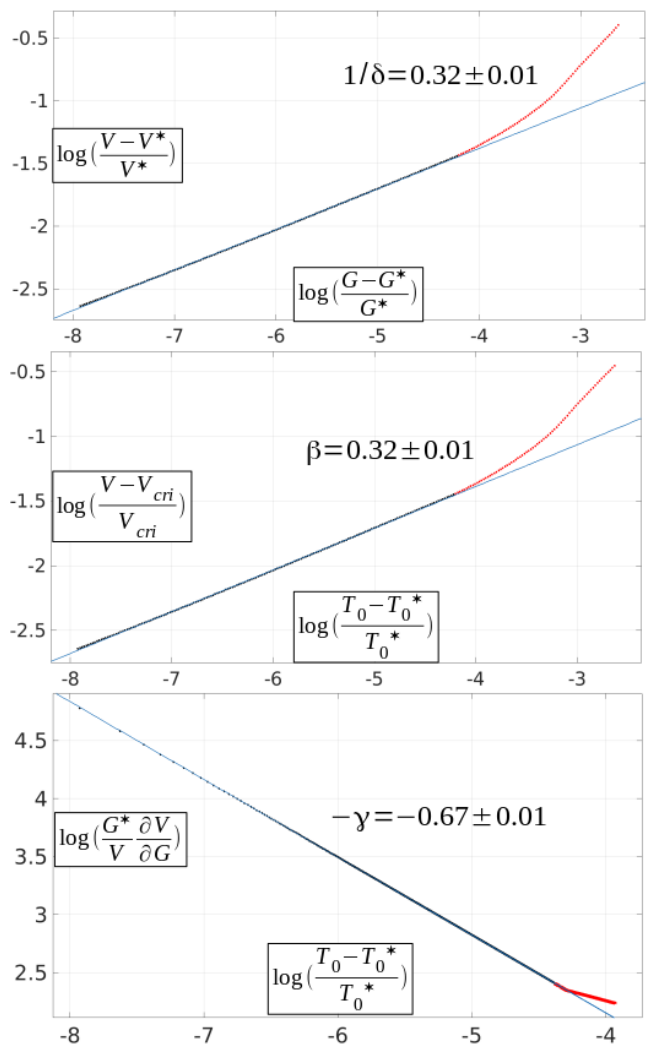


FIG. 4. Representation in the log-log domains (base 10) of the V surface (i.e., Fig. M4) along particular directions in the vicinity of the critical point. Black points were numerically derived from Eq. (M3) and the plain lines are the linear fits from which the red points were discarded. These fits are done beyond the critical point ($T_0 > T_0^*$).

they are fitted in the direct neighborhood of the CP. We thus had to refine the position of the critical point with an iterative inversion in the vicinity of the firstly estimated location. The principle was to find T_0^* and G^* in this vicinity such that the velocity range on which to fit the exponents is maximized. The chosen procedure was to: first derive an a priori exponent β_1 in a direct neighborhood of the first CP estimation, then chose a smaller vicinity in which to vary the CP position, compute for each of these positions a more local β_2 value, derive a new CP position by minimizing $|\beta_2 - \beta_1|$, iterate. Choosing smaller and smaller vicinities, this method allowed us to get a more accurate critical point and hence to expand the ranges on which to fit our final exponents. The corresponding decades and the respective exponents fits are

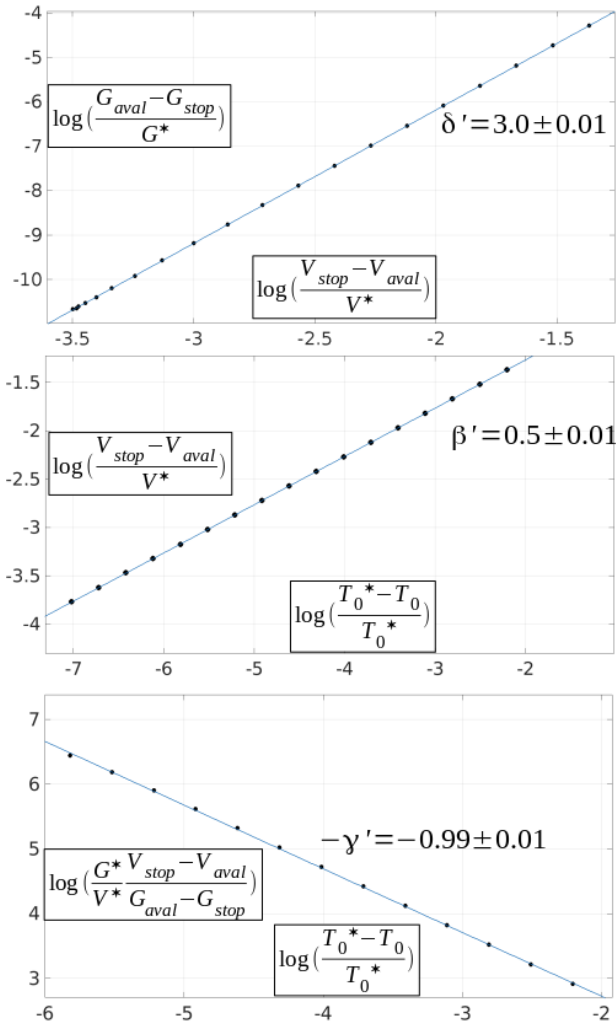


FIG. 5. Representation in the log-log domains (base 10) of the V surface (i.e., Fig. M4) along particular directions in the vicinity of the critical point. Black points were numerically derived from Eq. (M3) and the plain lines are the linear fits. These fits are done on the phase co-existence curve ($T_0 < T_0^*$).

shown in Fig. 4 and 5. We consider the reduced parameters $\Delta T_0/T_0^*$ and $\Delta G/G^*$, where $\Delta T_0 = T_0 - T_0^*$ and ΔG stands either for $G - G^*$ or $G_{\text{aval}} - G_{\text{stop}}$ depending on the exponents (see Eq. (M4) to (M9)). Varying these parameters, the fits of the crack velocity function extend on at least three and a half decades (for β , δ and γ) and up to five decades (for β' and δ').

-
- [1] O. Lengliné, R. Toussaint, J. Schmittbuhl, J. E. Elkhoury, J. P. Ampuero, K. T. Tallakstad, S. Santucci, and K. J. Måløy. Average crack-front velocity during subcritical fracture propagation in a heterogeneous medium. *Phys. Rev. E*, 84:036104, Sep 2011. doi:10.1103/PhysRevE.84.036104.
- [2] K. T. Tallakstad, R. Toussaint, S. Santucci, J. Schmittbuhl, and K. J. Måløy. Local dynamics of a randomly pinned crack front during creep and forced propagation: An experimental study. *Phys. Rev. E*, 83:046108, 04 2011.
- [3] L. B. Freund. Crack propagation in an elastic solid subjected to general loading. *Journal of the Mechanics and Physics of Solids*, 20(3):129 – 152, 1972. ISSN 0022-5096. doi:10.1016/0022-5096(72)90006-3.
- [4] A. Zerwer, M. A. Polak, and J. C. Santamarina. Wave propagation in thin plexiglas plates: implications for Rayleigh waves. *NDT and E International*, 33(1):33 – 41, 2000. ISSN 0963-8695. doi:10.1016/S0963-8695(99)00010-9.
- [5] G. G. Hammes. *Principles of Chemical Kinetics*. Academic Press, 1978. ISBN 978-0-12-321950-3. doi:doi.org/10.1016/B978-0-12-321950-3.50005-0.
- [6] Evonik Industries AG. Technical information, PLEXIGLAS GS/XT. 2013. URL <https://www.plexiglas.de/sites/lists/pm/documentsap/211-1-plexiglas-gs-xt-en.pdf>.
- [7] H. S. Carslaw and J. C. Jaeger. *Conduction of heat in solids*. 1959.
- [8] R. Toussaint, O. Lengliné, S. Santucci, T. Vincent-Dospital, M. Naert-Guillot, and K. J. Måløy. How cracks are hot and cool: a burning issue for paper. *Soft Matter*, 12:5563–5571, 2016. doi:10.1039/C6SM00615A.